

# CoFiI2P: Coarse-to-Fine Correspondences-Based Image-to-Point Cloud Registration

Shuhao Kang<sup>†</sup>, Youqi Liao<sup>†</sup>, Jianping Li, Fuxun Liang, Yuhao Li, Xianghong Zou, Fangning Li, Xieyuanli Chen, Zhen Dong, Bisheng Yang

**Abstract**— Image-to-point cloud (I2P) registration is a fundamental task for robots and autonomous vehicles to achieve cross-modality data fusion and localization. Existing I2P registration methods estimate correspondences at the point/pixel level, often overlooking global alignment. However, I2P matching can easily converge to a local optimum when performed without high-level guidance from global constraints. To address this issue, this paper introduces CoFiI2P, a novel I2P registration network that extracts correspondences in a coarse-to-fine manner to achieve the globally optimal solution. First, the image and point cloud data are processed through a Siamese encoder-decoder network for hierarchical feature extraction. Second, a coarse-to-fine matching module is designed to leverage these features and establish robust feature correspondences. Specifically, In the coarse matching phase, a novel I2P transformer module is employed to capture both homogeneous and heterogeneous global information from the image and point cloud data. This enables the estimation of coarse super-point/super-pixel matching pairs with discriminative descriptors. In the fine matching module, point/pixel pairs are established with the guidance of super-point/super-pixel correspondences. Finally, based on matching pairs, the transform matrix is estimated with the EPnP-RANSAC algorithm. Extensive experiments conducted on the KITTI dataset demonstrate that CoFiI2P achieves impressive results, with a relative rotation error (RRE) of 1.14 degrees and a relative translation error (RTE) of 0.29 meters. These results represent a significant improvement of 84% in RRE and 89% in RTE compared to the current state-of-the-art (SOTA) method. The project page is available at <https://whu-usi3dv.github.io/CoFiI2P>.

**Index Terms**— Image-to-Point Cloud Registration, Coarse-to-Fine Correspondence, Transformer Networks

## I. INTRODUCTION

Estimating six degrees of freedom (6-DoF) pose of a monocular image concerning a pre-build point cloud map is a fundamental requirement for robots and autonomous vehicles [1], [2]. Due to the limited onboard resources, robots are often equipped with only a monocular camera while facing challenges related to scale ambiguity in absolute localization and depth sensing. The establishment of a precise pose transformation between the image coordinate system and the

This study was jointly supported by the National Natural Science Foundation Project (No. 42201477, No. 42130105) and Open Fund of Key Laboratory of Urban Spatial Information, Ministry of Natural Resources (Grant No. 2023ZD001). (Shuhao Kang and Youqi Liao are co-first authors and contribute equally to the paper.) (Corresponding author : Jianping Li)

S. Kang is with the Technical University of Munich. Y. Liao is Wuhan University and Hubei Luojia Laboratory. Z. Dong, F. Liang, Y. Li, X. Zou and B. Yang are with Wuhan University. J. Li is with Nanyang Technological University. F. Li is with Beijing Urban Construction Exploration and Surveying Design Research Institute Co. Ltd. X. Chen is with the national university of defense technology, China.

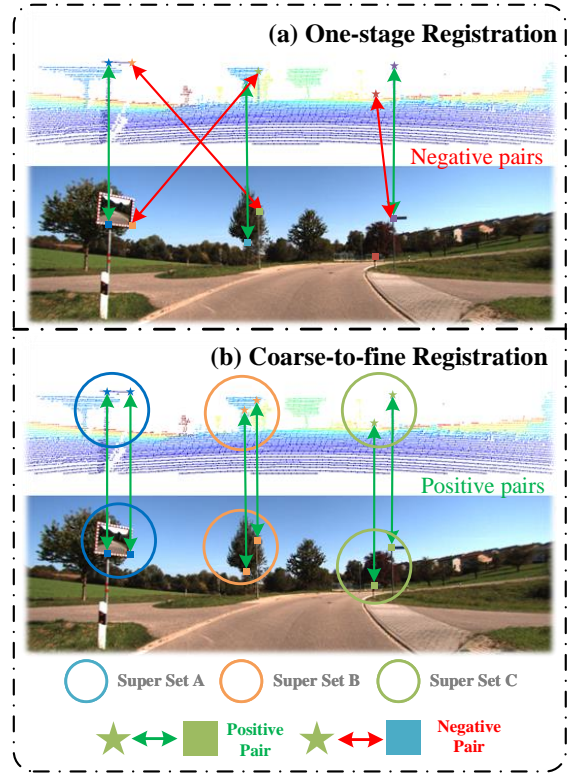


Fig. 1: Comparison of existing one-stage I2P registration scheme and proposed coarse-to-fine I2P registration scheme. (a) shows the one-stage registration pipeline, where matching pairs are directly established at the point/pixel level, leading to a significant number of mismatches. (b) shows our coarse-to-fine matching pipeline. Under the guidance of super point-to-pixel pairs, point-to-pixel pairs are generated from the existing super pairs, which effectively eliminates most mismatches.

pre-built point cloud coordinate system is important, as it not only accurately localizes the robot but also effectively reduces scale uncertainty inherent in monocular data [3].

However, cross-modality registration has its inherent challenges. Some existing methods use hand-crafted detectors and descriptors for I2P registration [4]. These approaches rely on structured features like edge features [5], which are limited by specific environmental conditions. With the rapid development of deep learning (DL), learning-based I2P registration approaches [6], [7], [8] have been proposed to extract representative keypoints and descriptors. However, the manually designed detectors for keypoints extraction lead to poor correspondence accuracy. To alleviate the difficulty of correspondence construction and improve the registration success rate, DeepI2P [7] converts the registration problem

to a classification problem. A novel binary classification network is designed to distinguish whether the projected points are within or beyond the camera frustum. The classification results are passed into an inverse camera projection solver to estimate the transformation between the camera and laser scanners. As a large number of points on the boundary are misclassified, the accuracy of the camera pose is still limited. CorriI2P [8] proposed an overlap region detector for both image and point cloud, then pixels and points in the overlap region are matched to obtain I2P correspondences. Feature fusion module is exploited to fuse the point cloud and image information. Although CorriI2P [8] has significant improvement over DeepI2P [7], matching merely on one stage, namely, the pixel-point level without global alignment guidance, can lead to local minimal and instability.

Inspired by recent coarse-to-fine matching schedules and transformers in image-to-image (I2I) registration [9], [10] and point cloud-to-point cloud (P2P) registration approaches [11], this paper proposes the **Coarse-to-Fine Image-to-Point** cloud (CoFiI2P) network to tackle the challenges of existing one-stage I2P registration. I2P transformer with self-attention modules and cross-attention modules is embedded into the network for global alignment. CoFiI2P mainly contains four modules: feature extraction (FE), coarse matching (CM), fine matching (FM), and pose estimation (PE). FE module embeds input image and point cloud into shared high-dimensional spaces, and then CM and FM modules establish super-point/super-pixel correspondences and point/pixel correspondences. In the PE module, the relative transformation between the camera and laser scanners is estimated with EPnP-RANSAC algorithm [12], [13]. Overall, the main contributions of this paper are:

- 1) A novel coarse-to-fine I2P registration network is proposed to align image and point cloud in a progressive way. The coarse matching step provides robust but rough super-point/super-pixel correspondences for the fine matching step, which filters out most mismatched pairs and reduces the computation burden. The fine matching step achieves accurate and reliable point/pixel correspondences within the global guidance.
- 2) A novel I2P transformer that incorporates both self-attention and cross-attention modules is proposed to enhance its global-aware capabilities in homogeneous and heterogeneous data. The self-attention module enables the capture of spatial context within the same modality data, while the cross-attention module facilitates the extraction of hybrid features from both the image and point cloud data.

## II. RELATED WORK

### A. Same-modality Registration

1) *I2I Registration*: before the age of deep-learning, hand-crafted detectors and descriptors (i.e., SIFT [14] and ORB [15]) are widely used to extract correspondences. Compared to traditional methods, learning-based methods

improve the robustness and accuracy of image matching with large viewpoint differences and illumination changes. SuperPoint [16] proposed a self-learning training method through homography adaptation. SuperGlue [17] proposed an attention-based graph neural network (GNN) for feature matching. Patch2Pix [18] is the first work to obtain patch matches and regress pixel-wise matches in a coarse-to-fine manner. LoFTR [9] operates detector-free matching to get dense correspondences and overcomes small receive field of CNN with transformer. However, I2I registration methods can not be directly transferred to the I2P registration, which extracts heterogeneous features from cross-modality data.

2) *P2P Registration*: point cloud registration aims to estimate the optimal rigid transformation of two point clouds. Correspondence-based methods [19], [20] estimate the correspondence first and recover the transformation with robust estimation methods [13]. RoReg [21] embeds orientation information of point cloud to estimate local orientation and refine coarse rotation through residual regression to achieve fine registration. In the transformer era, point-based transformers [11], [22] have emerged and shown great performance. CoFiNet [22] followed LoFTR's [9] design and proposed coarse-to-fine correspondences for registration, which computed coarse matches with descriptors strengthened by the transformer and refined coarse matches through density adaptive matching module. GeoTransformer [11] proposed a geometric Transformer to make full use of the 3D properties of the point cloud.

### B. Cross-modality Registration

To address the cross-modality registration problem, a variety of I2P registration methods have been proposed, which could be roughly divided into two categories: I2P fine registration (initial transformation dependent) and I2P coarse registration (initial transformation free). The I2P fine registration methods [4], [23], [24] rely on initial transform parameters, and are widely applied in sensors calibration. Although this paper focuses on the second class, namely the coarse I2P registration without any initial transformation knowledge, we give an exhaustive review of both categories registration methods here.

1) *Fine registration methods*: fine registration methods have been thoroughly researched for several decades. Early-stage studies [25], [26] utilize various artificial targets as calibration constraints. In recent years, some approaches have argued that structured features shared in images and point cloud could be used for target-less I2P registration, e.g., edge feature [23] and line feature [4]. [23] employs edge information and optimizes transformation according to the response value. [4] extracts lines from image and point clouds for registration. Recently, research on 2D and 3D semantic segmentation motivates semantic feature-based I2P registration. Se-calib [24] further studied semantic edges in I2P registration to employ more common semantic information instead of a certain type of object. Overall, fine registration methods achieve high accuracy but depend on the quality of the initial transformation value.

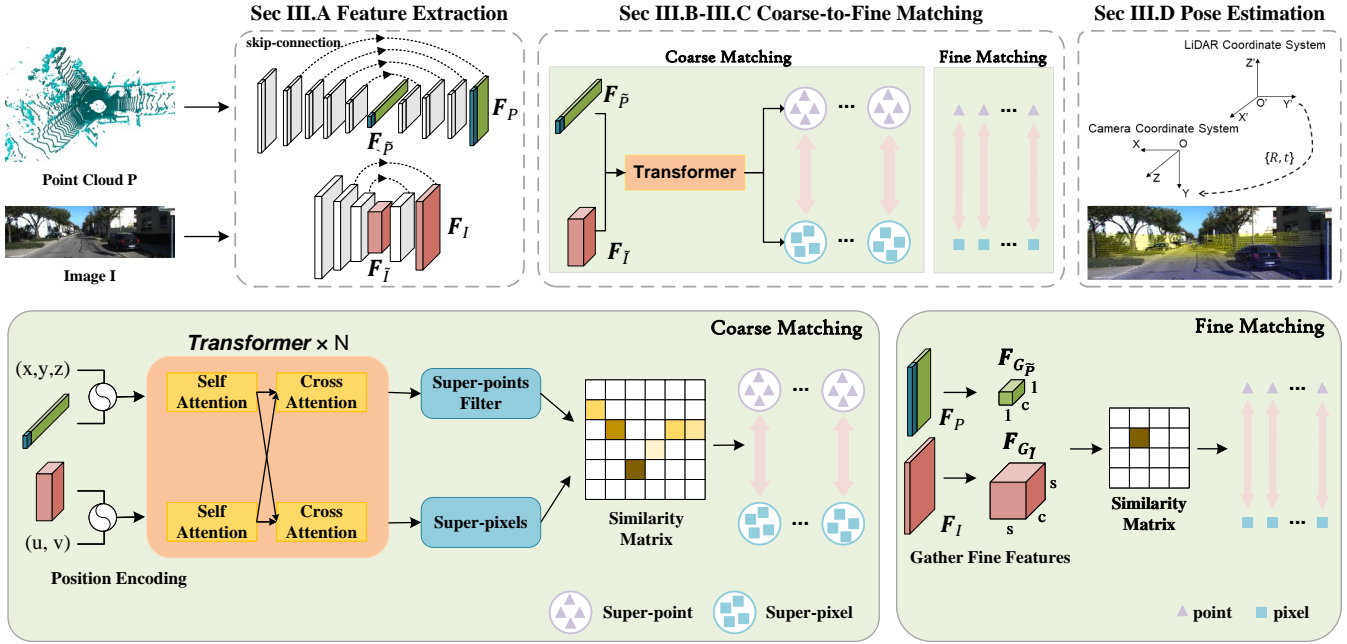


Fig. 2: Workflow of CoFiI2P. The proposed method consists of feature extraction, coarse matching, fine matching and pose estimation modules. Image and point cloud are sent to the feature extraction module to obtain hierarchical deep features, respectively. The coarse-level features are strengthened by I2P transformer module and then matched with the cosine similarity rule. Fine features are gathered from the last layer of the decoder. In each super-point/super-pixel pair, the node point is set as the candidate and the corresponding pixel is selected from the super-pixel area, a  $s \times s$  window. The generated dense matching pairs are utilized to regress the pose with the EPnP-RANSAC [12], [13] algorithm.

2) *Coarse registration methods*: 2D3D-Matchnet [6] is the pioneering method to regress the relative transform parameters with CNN. It extracts SIFT [14] and ISS [27] keypoints from image and point cloud and learns descriptors with a Siamese network. However, the hand-crafted detectors from different modalities match poorly. DeepI2P [7] proposed a feature fusion module to merge image and point cloud information and classify points in/beyond the camera frustum. CorrI2P [8] predicts pixels and points in overlapping areas and matches with dense per-pixel/per-point features directly to get I2P correspondences. Although overlapping region detectors significantly reduce the number of false candidates, I2P registration only using the low-level feature without global guidance leads to serious mismatches. Inspired by the coarse-to-fine strategies in CoFiNet [22], we propose the coarse-to-fine I2P registration network CoFiI2P, which injects the information of high-level correspondences into low-level matching for rejecting mismatches.

### III. METHODOLOGY

For convenient description, a pair of partially overlapped image and point cloud are defined as  $I \in \mathbb{R}^{W \times H \times 3}$  and  $P \in \mathbb{R}^{N \times 3}$ , where  $W$  and  $H$  are the width and height, and  $N$  is the number of points. The purpose of I2P registration is to estimate the relative transformation between the image  $I$  and point cloud  $P$ , including rotation matrix  $\mathbf{R} \in \mathbb{R}^{3 \times 3}$  and translation vector  $\mathbf{t} \in \mathbb{R}^3$ .

Our method adopts the coarse-to-fine manner to find the correct correspondences set  $\Omega(I, P)$ . The CoFiI2P mainly consists of four modules: feature extraction (FE), coarse matching (CM), fine matching (FM) and pose estimation

(PE). FE is an encoder-decoder structure network, that encodes raw inputs from different modalities into high-dimension feature spaces and finds in-frustum super-points. CM and FM are cascaded two-stage matching modules. CM constructs coarse matching at super-pixel/super-point level, and then FM constructs fine matching at pixel/point level sequentially with the guidance of super-pixel/super-point correspondences. Lastly, the PE module exploits point-pixel matching pairs to regress the relative pose with EPnP-RANSAC [12], [13] algorithm. The workflow of the proposed method is shown in Fig. 2.

#### A. Multi-scale Feature extraction

We utilize ResNet-34 [28] and KPConv-FPN [29] as the backbones for image and point cloud to extract multi-level features. The encoder progressively embeds raw inputs into high-dimensional features, and the decoder propagates high-level information to low-level details with skip-connection for dense per-pixel/point feature generation. Then, we extract features from multiple resolutions for coarse-to-fine matching. Specifically, super-points set  $\tilde{P}$  and super-pixels set  $\tilde{I}$  at the coarsest resolution are chosen as candidates for coarse matching, and local points group  $G_{\tilde{P}}$  and pixels patches  $G_{\tilde{I}}$  are generated from coarse matching pairs for fine matching. The local points group  $G_{\tilde{P}_x}$  are constructed with the point-to-node strategy in the geometric space:

$$G_{\tilde{P}_x} = \{p \in P \mid \|p - \tilde{p}_x\| < r_g\}, \quad (1)$$

where  $r_g$  is the chosen radius. As the pixels array on the image with a rigid order, the local pixels patch  $G_{\tilde{I}}$  construct simply with the pyramid matching strategy.

## B. I2P Coarse Matching

In CM module, I2P transformer is utilized to capture the geometric and spatial consistency between image and point cloud. Each stage of the I2P transformer consists of a self-attention block for inter-modality long-range context and a cross-attention module for intra-modality feature exchange. The self-attention and cross-attention modules are repeated several times to extract well-mixed features for super-point/super-pixel correspondence matching.

1) *I2P Transformer*: [30], [31] have shown that Vision Transformer (ViT) outperforms traditional CNN-based methods with a large margin in classification, detection, segmentation and other downstream tasks. Furthermore, recent approaches [9], [10], [32] have introduced transformer modules for I2I and P2P registration tasks. Therefore, we introduce the I2P transformer module customized for cross-modality registration task to enhance the representability and robustness of descriptors. Different from ViT used in the same-modality registration tasks, our I2P transformer contains both self-attention modules for space context capturing in homogeneous data and cross-attention for hybrid feature extraction among heterogeneous data.

For the self-attention module, given a coarse-level feature map  $\mathbf{F} \in \mathbb{R}^{N \times C}$  of image or point cloud, the query, key and value vectors  $\mathbf{q}, \mathbf{k}, \mathbf{v}$  are generated as:

$$\mathbf{q} = \mathbf{W}_q \mathbf{F}, \mathbf{k} = \mathbf{W}_k \mathbf{F}, \mathbf{v} = \mathbf{W}_v \mathbf{F}, \quad (2)$$

where  $\mathbf{W}_q, \mathbf{W}_k \in \mathbb{R}^{C_{qk}^{sa} \times C}, \mathbf{W}_v \in \mathbb{R}^{C_v^{sa} \times C}$  are learnable weight matrixs. Then, the global attention enhanced feature map  $\mathbf{F}^{sa}$  is calculated as:

$$\mathbf{F}^{sa} = \text{Softmax}\left(\frac{\mathbf{q}\mathbf{k}^\top}{\sqrt{C}}\right)\mathbf{v}. \quad (3)$$

Extracted global-aware features  $\mathbf{F}^{sa}$  are fed into the feed-forward network (FFN) to fuse the spatial relation information in channel dimension. Given a feature map  $\mathbf{F}$ , the relative positions are encoded with multi-layer perception (MLP) [33].

Cross-attention is designed for fusing image and point cloud features in I2P registration task. Given the feature map  $\mathbf{F}_{\tilde{P}}, \mathbf{F}_{\tilde{I}}$  for super-points set  $\tilde{P}$  and super-pixels set  $\tilde{I}$ , cross-attention enhanced feature maps  $\mathbf{F}_{\tilde{P}}^{ca}$  of point cloud and  $\mathbf{F}_{\tilde{I}}^{ca}$  of image are calculated as:

$$\begin{aligned} \mathbf{F}_{\tilde{P}}^{ca} &= \text{Softmax}\left(\frac{\mathbf{q}_{\tilde{P}}\mathbf{k}_{\tilde{I}}^\top}{\sqrt{C}}\right)\mathbf{v}_{\tilde{P}}, \\ \mathbf{F}_{\tilde{I}}^{ca} &= \text{Softmax}\left(\frac{\mathbf{q}_{\tilde{I}}\mathbf{k}_{\tilde{P}}^\top}{\sqrt{C}}\right)\mathbf{v}_{\tilde{I}}, \end{aligned} \quad (4)$$

where  $\mathbf{q}_{\tilde{P}}, \mathbf{k}_{\tilde{P}}, \mathbf{v}_{\tilde{P}}$  are query, key and value vectors of point cloud feature  $\mathbf{F}_{\tilde{P}}$ , and  $\mathbf{q}_{\tilde{I}}, \mathbf{k}_{\tilde{I}}, \mathbf{v}_{\tilde{I}}$  are query, key and value vectors of image feature  $\mathbf{F}_{\tilde{I}}$ .

**Remark.** While the self-attention module encodes the spatial and geometric features for each super-pixel and super-point, the cross-attention module injects the geometric structure information and texture information across image and point cloud respectively. Outputs of the I2P transformer carry powerful cross-modality information for matching.

2) *Super-point/Super-pixel Matching*: for the monocular camera, the field of view (FoV) is obviously smaller than the laser scans of 3D Lidar (e.g., Velodyne-H64), which usually sweeps 360 degrees in the horizontal direction. Therefore, only a small number of super-points are in the camera frustum. To filter out beyond-frustum super-points, we add a simple binary classification head to predict super-points in or beyond the frustum of the camera. After the beyond-frustum super-points are removed, the coarse level correspondences are estimated between in-frustum super-points set  $\tilde{P}$  and super-pixels set  $\tilde{I}$  by sorting the nearest super-pixel  $\tilde{i}$  in feature space:

$$\tilde{\Omega}_{\mathcal{M}} = \{(\tilde{p}_x \in \tilde{P}, \tilde{i}_y \in \tilde{I}) | y = \underset{|\tilde{I}|}{\text{argmin}} \|\mathbf{F}_{\tilde{P}}(\tilde{p}_x) - \mathbf{F}_{\tilde{I}}(\tilde{i}_y)\|\}, \quad (5)$$

where  $\mathbf{F}_{\tilde{P}}$  and  $\mathbf{F}_{\tilde{I}}$  are corresponding feature maps.

## C. I2P Fine Matching

The first-stage matching at the coarse level constructs coarse super-point/super-pixel pairs  $\tilde{\Omega}_{\mathcal{M}}$  but leads to poor registration accuracy. In order to obtain high-quality I2P correspondences, we generate fine correspondence based on the coarse matching results. During the decoder process, in each super-point/super-pixel correspondence  $(\tilde{p}_x, \tilde{i}_y)$ , the super-point  $\tilde{p}_x$  reverse to local points group  $G_{\tilde{p}_x}$  and the super-pixel  $\tilde{i}_y$  reverse to local pixels patch  $G_{\tilde{i}_y}$ . Considering the uneven distribution of point cloud and computational efficiency, only the node points  $p_n$  in local patch group  $G_{\tilde{p}}$  are selected to establish correspondences. For each node point  $p_n$ , we select the pixel  $i_k \in G_{\tilde{i}_y}$  that lies nearest in the feature space. Point-pixel pairs in each super-point-super-pixel pair are staked together as the dense corresponding pairs  $\Omega_{\mathcal{M}}$ . With point feature map  $\mathbf{F}_{G_{\tilde{p}}}$  and pixel feature map  $\mathbf{F}_{G_{\tilde{i}}}$  of local patch, the fine matching process is defined as:

$$\Omega_{\mathcal{M}} = \{(p_n \in G_{\tilde{p}}, i_k \in G_{\tilde{i}}) | k = \underset{|G_{\tilde{i}}|}{\text{argmin}} \|\mathbf{F}_{G_{\tilde{p}}}(p_n) - \mathbf{F}_{G_{\tilde{i}}}(i_k)\|\}\}. \quad (6)$$

## D. EPnP-RANSAC based Pose Estimation

With the precise point-pixel pairs  $\Omega_{\mathcal{M}}$ , the relative transformation can be solved with EPnP [12] algorithm. As mentioned in previous approaches, wrong matching may infiltrate into the point-pixel pairs and decrease the registration accuracy. In the CoFiI2P, EPnP-RANSAC [12], [13] algorithm is used for robust estimating camera relative pose.

## E. Loss Function

In order to supervise the network simultaneously learning coarse level descriptors, fine level descriptors and in/beyond-frustum super-points classification, we introduce a joint loss function consisting of coarse level descriptor loss  $\mathcal{L}_{coarse}$ , fine level descriptor loss  $\mathcal{L}_{fine}$  and classification loss  $\mathcal{L}_{classify}$ . The classification loss encourages the network to correctly label each super-point, and two descriptor losses pull positive matching pairs closer and push negative matching pairs farther in feature space.

The cosine similarity rule  $s(p_x, i_y)$  of point cloud feature vector  $\mathbf{F}(p_x)$  and image feature vector  $\mathbf{F}(i_y)$  is defined as :

$$s(p_x, i_y) = \frac{\langle \mathbf{F}(p_x), \mathbf{F}(i_y) \rangle}{\|\mathbf{F}(p_x)\| \|\mathbf{F}(i_y)\|}, \quad (7)$$

and the distance  $d(p_x, i_y)$  is defined as:

$$d(p_x, i_y) = 1 - s(p_x, i_y). \quad (8)$$

On the coarse level, the positive anchor  $\tilde{i}_{pos}$  for each in-frustum super-point  $\tilde{p}_x$  is sampled from the ground-truth pairs set  $\tilde{\Omega}_{\mathcal{M}^*}$ :

$$\tilde{\Omega}_{\mathcal{M}^*} = \{(\tilde{p}_x \in \tilde{P}, \tilde{i}_{pos} \in \tilde{I}) | \tilde{i}_{pos} = \Gamma(\mathbf{T}\tilde{p}_x)\}, \quad (9)$$

where  $\mathbf{T}$  is the ground-truth transform matrix from point cloud coordinate system to image frustum coordinate system, and  $\Gamma$  represents the mapping function that converts points from camera frustum to image plane coordinate system. The negative anchor  $\tilde{i}_{neg}$  is defined as the super-pixel with the smallest distance to the  $\tilde{p}_x$  in the feature space:

$$\tilde{i}_{neg} = \underset{\tilde{i} \in \tilde{I}}{\operatorname{argmin}} \|d(\tilde{p}_x, \tilde{i}_{neg})\| \quad \text{s.t.} \quad \|\tilde{i}_{neg} - \tilde{i}_{pos}\| > r, \quad (10)$$

where  $r$  is the safe radius to remove adversarial samples. Finally, with positive margin  $\Delta_{pos}$  and negative margin  $\Delta_{neg}$ , coarse level descriptor loss is defined in a triplet way as Eq. (11) :

$$\mathcal{L}_{coarse} = \sum_{(\tilde{p}_x, \tilde{i}_{pos}, \tilde{i}_{neg})} \left( \max(0, d(\tilde{p}_x, \tilde{i}_{pos}) - \Delta_{pos}) + \max(0, \Delta_{neg} - d(\tilde{p}_x, \tilde{i}_{neg})) \right). \quad (11)$$

Fine level descriptor loss is defined as modified circle loss [34]. We randomly select  $n$  in-frustum point and their positive anchor pixels and negative anchors, as Eq. (10), then the descriptor loss is defined as:

$$\mathcal{L}_{fine} = \log \left( 1 + \exp(-\gamma \alpha_{pos}(s(p_x, i_{pos}) - \Delta_{pos})) + \sum_{(p_x, i_{pos}, i_{neg})} \exp(\gamma \alpha_{neg}(s(p_x, i_{neg}) - \Delta_{neg})) \right), \quad (12)$$

where  $\alpha_{neg}$  and  $\alpha_{pos}$  are the dynamic optimizing rates towards negative and positive pairs, and  $\gamma$  is the scale factor. As in [34], the  $\alpha_{neg}$  and  $\alpha_{pos}$  are defined as:

$$\begin{aligned} \alpha_{neg} &= \max(0, s(p_x, i_{neg}) + \Delta_{neg}), \\ \alpha_{pos} &= \max(0, 1 + \Delta_{pos} - s(p_x, i_{pos})). \end{aligned} \quad (13)$$

Super-points classification loss is a binary cross-entropy loss:

$$\mathcal{L}_{classify} = - \sum_{\tilde{p}_x \in \tilde{P}} (\tilde{p}_x \log(\tilde{p}_x^*) + (1 - \tilde{p}_x) \log(1 - \tilde{p}_x^*)). \quad (14)$$

Overall, our loss function is

$$\mathcal{L} = \lambda_1 \mathcal{L}_{coarse} + \lambda_2 \mathcal{L}_{fine} + \lambda_3 \mathcal{L}_{classify}, \quad (15)$$

where  $\lambda_1, \lambda_2, \lambda_3$  are hyperparameters that control the weights between losses.

## IV. EXPERIMENTS

### A. Experiment setup

1) *Dataset*: we evaluate our method on KITTI Odometry dataset [35], a benchmark dataset extensively employed in the field of I2P registration. KITTI Odometry dataset consists of 22 sequences of images and point cloud data collected simultaneously in urban environments, encompassing a variety of road scenes and environmental conditions, and 11 sequences provide ground-truth calibration files. The camera intrinsic function  $\Gamma$  extracted from calibration files is thought unbiased during experiments. For a fair comparison with existing approaches [7], [8], sequences 0-8 are used for training and 9-10 for testing.

2) *Baseline methods*: we compare proposed CoFiI2P with two open-sourced I2P methods:

- DeepI2P [7]: proposed the frustum classification and inverse camera projection to estimate the camera pose. Due to the time-consuming data pre-processing and training, we reference the registration results reported in the paper.
- CorrI2P [8]: is SOTA comparable I2P method. CorrI2P [8] predicts the overlapping area and establishes correspondences densely for pose estimation. We use officially released codes to reimplement this method. The only difference is the number of points changed from 40960 to 20480 for fair comparison.

3) *Evaluation metrics*: we report the relative rotation error (RRE), relative translation error (RTE) and registration recall (RR) to evaluate the registration results. Inlier ratio (IR) and root mean square error (RMSE) used in I2P and P2P approaches [22], [36] are introduced to evaluate the quality of correspondences. RRE and RTE are defined as :

$$\text{RRE} = \sum_{i=1}^3 |\mathbf{r}(i)|, \quad \text{RTE} = \|\mathbf{t}_{gt} - \mathbf{t}_e\|, \quad (16)$$

where  $\mathbf{r}$  is the Euler angle vector of  $\mathbf{R}_{gt}^{-1} \mathbf{R}_e$ ,  $\mathbf{R}_{gt}$  and  $\mathbf{t}_{gt}$  are the ground-truth rotation and translation matrix,  $\mathbf{R}_e$  and  $\mathbf{t}_e$  are the estimated rotation and translation matrix.

RR metric [22], [36] estimates the percentage of correctly matched pairs, indicating the descriptor learning ability of networks. RR is defined as:

$$\text{RR}_{\mathcal{M}} = \frac{1}{|\Omega_{\mathcal{M}}|} \sum_{i=1}^{|\Omega_{\mathcal{M}}|} \mathbb{1} \left( \sqrt{\frac{1}{|\Omega_{\mathcal{M}}|} \sum_{(p_x, i_y) \in \Omega_{\mathcal{M}}} \|\Gamma(\mathbf{T}p_x) - i_y\|} < \tau \right), \quad (17)$$

$\tau$  is the threshold to remove false registration results, i.e.  $10^\circ/5m$ . IR denotes the inlier ratio of matching pairs, which measures the accuracy of correspondences. The IR for point/pixel correspondences set  $\Omega_{\mathcal{M}}$  is defined as :

$$\text{IR}_{\mathcal{M}} = \frac{1}{|\Omega_{\mathcal{M}}|} \sum_{(p_x, i_y) \in \Omega_{\mathcal{M}}} \mathbb{1} (\|\Gamma(\mathbf{T}p_x) - i_y\| < \tau), \quad (18)$$

in which  $\tau$  is used to control the reprojection error tolerance. RMSE denotes the average reprojection error over the

correspondences set  $\Omega_{\mathcal{M}}$ :

$$\text{RMSE}_{\mathcal{M}} = \sqrt{\frac{1}{|\Omega_{\mathcal{M}}|} \sum_{(p_x, i_y) \in \Omega_{\mathcal{M}}} \|\Gamma(\mathbf{T}p_x) - i_y\|}. \quad (19)$$

## B. Implementation Details

Raw images and point clouds are preprocessed to filter out noise and reduce the computational burden. The top 50 rows of images are cropped out as most of these pixels see the sky. Then images are resized to  $512 \times 160$  for training and testing. The points are downsampled with  $0.1m \times 0.1m \times 0.1m$  voxel and then randomly sampled 20480 points as input.

During the training process, with correct transform parameters provided by the calibration files, the ground truth correspondences  $\Omega_{\mathcal{M}^*}$  are established to supervise the network. We trained the whole network 25 epochs with batch size of 1. We use the Adam to optimize the network, and the initial learning rate is 0.001 and multiple by 0.25 after every 5 epochs. For our joint loss, we set  $\lambda_1 = \lambda_2 = \lambda_3 = 1$ . The safe radius  $r$ , positive margin  $\Delta_{pos}$  and negative margin  $\Delta_{neg}$  in loss function are set to 1, 0.2 and 1.8 respectively. Scale factor  $\gamma$  is set to 10. During the coarse matching, super-points are projected to the frustum of the image, and beyond-frustum super-points are removed. Then we uniformly sample 64 super-points from in-frustum ones. The corresponding super-pixels are found with Eq. 4. The training of CoFiI2P takes about 49 hours. During the testing process, we set the confidence threshold as 0.9 to obtain reliable in-frustum super-points in coarse matching. All the experiments are conducted on a single RTX 4090 GPU.

TABLE I: Registration accuracy on KITTI dataset

	Threshold( $^{\circ}/m$ )	RRE( $^{\circ}$ ) $\downarrow$	RTE(m) $\downarrow$	RR(%) $\uparrow$
DeepI2P (2D)	10/5	$7.56 \pm 7.63$	$3.28 \pm 3.09$	-
DeepI2P (3D)	10/5	$15.52 \pm 12.73$	$3.17 \pm 3.22$	-
	none/none	$6.93 \pm 29.03$	$2.68 \pm 10.51$	-
CorrI2P	45/10	$3.41 \pm 3.64$	$1.48 \pm 1.35$	97.07
	10/5	$2.70 \pm 1.97$	$1.24 \pm 0.87$	90.66
	none/none	<b><math>1.14 \pm 0.78</math></b>	<b><math>0.29 \pm 0.19</math></b>	-
CoFiI2P	45/10	<b><math>1.14 \pm 0.78</math></b>	<b><math>0.29 \pm 0.19</math></b>	<b>100.00</b>
	10/5	<b><math>1.14 \pm 0.78</math></b>	<b><math>0.29 \pm 0.19</math></b>	<b>100.00</b>

## C. Registration Accuracy

We report the RRE and RTE of our CoFiI2P as registration evaluation metrics under three different settings in Table I, where *none/none* means no specific thresholds for filtering out false registration frames and  $10^{\circ}/5m$  and  $45^{\circ}/10m$  mean that any frames with registration errors exceeding these specified thresholds are ignored during the evaluation process. By employing these diverse settings, we can conduct a more equitable analysis. As shown in Table I, the proposed method outperforms all baseline methods by a large margin. Specifically, with different registration error threshold *none/none*,  $45^{\circ}/10m$ ,  $10^{\circ}/5m$ , the RRE reduces 84%, 67%, 58% and the RTE reduces 89%, 80%, 77% compared to CorrI2P [8] respectively. Meanwhile, the RR improves by 2.93%, 9.34% under two pairs of thresholds. Notably, our method achieves 100% RR even under hardest pair of thresholds  $10^{\circ}/5m$ , which indicates that our method

achieves both robust and accurate performance in all the evaluation scenes. Furthermore, we project the points to the image plane with transform parameters provided by ground-truth files, CorrI2P [8] and CoFiI2P respectively and deploy the qualitative registration results in Fig. 5. It can be seen that the CoFiI2P remains stable and provides more accurate results, which confirms our claim.

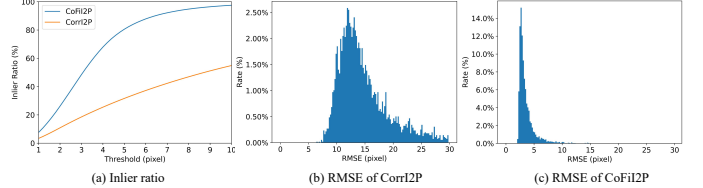


Fig. 3: Quantitative results of correspondences. (a) shows the inlier ratio, while (b) and (c) show the RMSE distribution of the CorrI2P and our CoFiI2P.

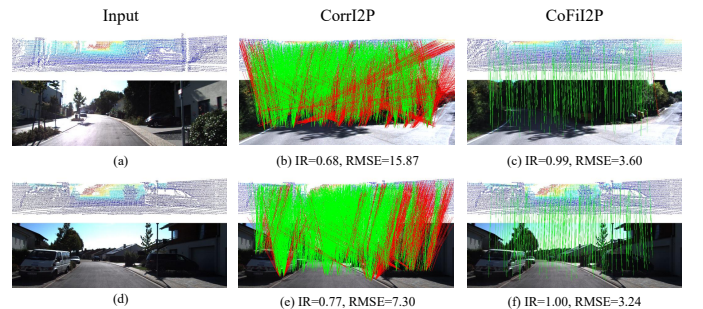
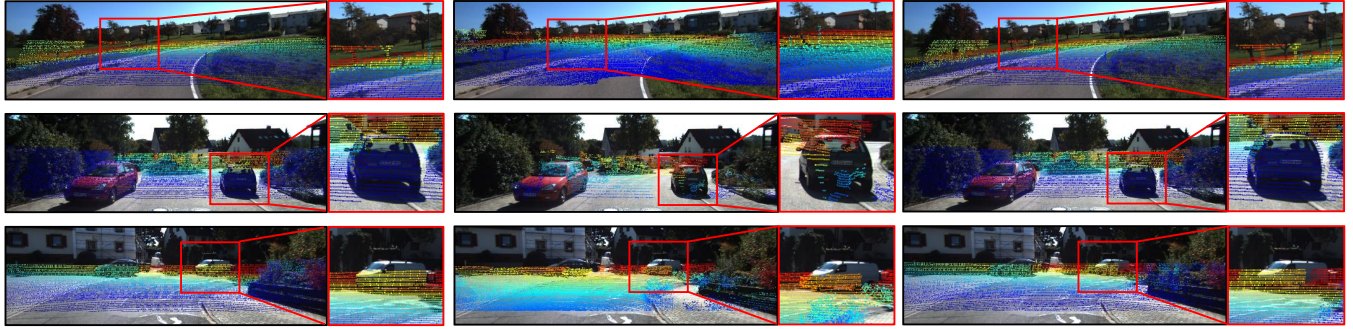


Fig. 4: Qualitative results of correspondences. The first column shows the input, and the second and third column shows the correspondences of CorrI2P and our CoFiI2P respectively. The green lines represent correct matches, while the red lines represent incorrect matches.

For the super-point frustum classification, the precision and recall of our method are 91.23% and 99.75% on the KITTI dataset, respectively. However, these numbers can not directly measure the quality of the correspondence. Therefore, we introduce the IR and RMSE metrics as in P2P registration approach [22] and show the results in Fig. 3 and Fig. 4. Fig. 3 (a) shows that CoFiI2P gets obviously higher IR scores than CorrI2P [8] under various thresholds, while Fig. 3 (b) and (c) demonstrate that our CoFiI2P owns higher correspondence accuracy. Specifically, CoFiI2P reduces the global average RMSE value from 30.35 pixels of CorrI2P [8] (seriously affected by the outliers with RMSE higher than 100 pixels) to 3.58 pixels. Fig. 4 shows that our CoFiI2P provides much cleaner correspondences set for pose estimation.

## D. Ablation studies and Insights

In this part, we analyze three crucial factors in our CoFiI2P: I2P transformer module, coarse-to-fine matching scheme and point cloud density. We conduct ablation studies on them to prove the effectiveness of each module and review the influence of point cloud density. In order to reduce the computational burden, we train the variant networks 10 epochs in the discussion part, instead of 25 epochs in the experiments part. We report the global RRE and RTE as evaluation metrics and no thresholds are used to reject false registration scenes.



(a) Ground Truth

(b) CorrI2P

(c) CoFiI2P

Fig. 5: Quantitative registration results. The colors are rendered based on depth, ranging from blue in the foreground to red in the distance.

1) *Analyze of the I2P transformer*: I2P transformer [37] with self-attention module and cross-attention module is crucial to image-to-point cloud alignment at the global level. In this part, we conduct ablation studies to assess the effectiveness of the I2P transformer. We train the CoFiI2P without any attention module as baseline. Then, the self-attention modules and cross-attention modules are added on the coarse level respectively. As shown in Table II, the baseline method performance drops significantly without any attention module. Besides, the self-attention module reduces the RRE about  $1.06^\circ$  and the RTE about  $0.47m$ , and the cross-attention module reduces the RRE about  $0.92^\circ$  and the RTE about  $0.38m$  respectively. With both the self-attention and cross-attention modules, the CoFiI2P achieves the smallest registration error. Moreover, with both self-attention and cross-attention modules, the variance reduces by a large margin, which indicates that the I2P transformer block enhances both the accuracy and robustness.

TABLE II: Ablation study on I2P transformer blocks. **SA** denotes self-attention module and **CA** denotes cross-attention module.

Baseline	SA	CA	RRE( $^\circ$ )	RTE(m)
✓			$2.88 \pm 5.32$	$0.90 \pm 2.44$
✓	✓		$1.82 \pm 2.71$	$0.43 \pm 0.75$
✓		✓	$1.96 \pm 1.95$	$0.52 \pm 0.59$
✓	✓	✓	<b><math>1.28 \pm 0.94</math></b>	<b><math>0.33 \pm 0.23</math></b>

2) *Analyze of the coarse-to-fine matching scheme*: our CoFiI2P proposes to estimate coarse correspondences at super-point-/pixel level first and then generate dense correspondences at point-pixel level sequentially. To demonstrate that the progressive two-stage registration operates better than the one-stage registration used in previous I2P approaches, we conduct ablation experiments on the coarse-to-fine matching scheme. This ablation study employs the backbone with full I2P transformer blocks as baseline and evaluates the registration accuracy with only the coarse matching scheme or fine matching scheme. For coarse matching only, the matching pairs are established on the coarse level and remapped to the original resolution for pose estimation. By contrast, for fine matching only, matching pairs are established on the fine level directly, without guidance of coarse level correspondences. Experiment results in Table III show that removing either coarse matching stage or fine matching stage leads to higher registration error and variance. We indicate that coarse-level registration provides robust

correspondences and fine-level registration provides accurate matching pairs. Combining the coarse-level and fine-level registration sequentially makes it easier to access the global optimal solution in I2P registration.

TABLE III: Ablation study on coarse-to-fine matching scheme. **CM** denotes coarse matching and **FM** denotes fine matching.

Baseline	CM	FM	RRE( $^\circ$ )	RTE(m)
✓	✓		$1.58 \pm 1.64$	$0.41 \pm 0.39$
✓		✓	$1.62 \pm 2.89$	$0.44 \pm 0.82$
✓	✓	✓	<b><math>1.28 \pm 0.94</math></b>	<b><math>0.33 \pm 0.23</math></b>

3) *Analysis of the point cloud density*: given the significant impact of point cloud density on representative learning, we conducted ablation studies to examine this influence. The results in Table IV present registration accuracy and computational complexity for various point cloud densities. All experimental settings and hyperparameters remained consistent with those outlined in Section IV-A. The findings in Table IV reveal that as point cloud density decreases, the qualitative metrics deteriorate, while higher point cloud densities correspond to a sharp increase in computational complexity. It's an intuitive observation that low-density point clouds lose local structured information, and high-density point clouds place a heavy computational burden. As a result, we opted for a compromise and selected 20480 points, striking a balance between efficiency and accuracy.

TABLE IV: Ablation study on point cloud density.

#Points	RRE( $^\circ$ )	RTE(m)	FLOPs
5120	$10.68 \pm 31.69$	$3.42 \pm 22.85$	37.42G
10240	$1.67 \pm 2.07$	$0.42 \pm 0.41$	56.00G
20480	$1.28 \pm 0.94$	$0.33 \pm 0.23$	93.80G
40960	$1.23 \pm 1.30$	$0.32 \pm 0.28$	171.91G

## V. CONCLUSION

In this paper, we propose CoFiI2P, a novel network for I2P registration. The core is the coarse-to-fine matching strategy, which establishes robust correspondence on the global level first and learns the precise correspondences on the local level progressively. Furthermore, the I2P transformer with self-attention and cross-attention module is introduced to enhance the global-aware ability in homogeneous and heterogeneous data. Compared with one-stage dense prediction and matching approaches, CoFiI2P filters out a large number of false correspondences and holds a safe lead in all the metrics. Extensive experiments on the KITTI dataset have demonstrated that CoFiI2P owns accuracy, robustness, and

efficiency in various environments. We hope that the released code of CoFi2P could motivate the related societies.

## REFERENCES

- [1] L. Wang, X. Zhang, W. Qin, X. Li, J. Gao, L. Yang, Z. Li, J. Li, L. Zhu, H. Wang *et al.*, “Camo-mot: Combined appearance-motion optimization for 3d multi-object tracking with camera-lidar fusion,” *IEEE Trans. on Intelligent Transportation Systems (T-ITS)*, 2023.
- [2] J. Li, S. Yuan, M. Cao, T.-M. Nguyen, K. Cao, and L. Xie, “Hcto: Optimality-aware lidar inertial odometry with hybrid continuous time optimization for compact wearable mapping system,” *ISPRS Journal of Photogrammetry and Remote Sensing (ISPRS)*, vol. 211, pp. 228–243, 2024.
- [3] X. Yan, J. Gao, C. Zheng, C. Zheng, R. Zhang, S. Cui, and Z. Li, “2dpss: 2d priors assisted semantic segmentation on lidar point clouds,” in *Proc. of the Europ. Conf. on Computer Vision (ECCV)*. Springer, 2022, pp. 677–695.
- [4] X. Zhang, S. Zhu, S. Guo, J. Li, and H. Liu, “Line-based automatic extrinsic calibration of lidar and camera,” in *Proc. of the IEEE Intl. Conf. on Robotics & Automation (ICRA)*, 2021, pp. 9347–9353.
- [5] C. Yuan, X. Liu, X. Hong, and F. Zhang, “Pixel-level extrinsic self calibration of high resolution lidar and camera in targetless environments,” *IEEE Robotics and Automation Letters (RA-L)*, vol. 6, no. 4, pp. 7517–7524, 2021.
- [6] M. Feng, S. Hu, M. H. Ang, and G. H. Lee, “2d3d-matchnet: Learning to match keypoints across 2d image and 3d point cloud,” in *Proc. of the IEEE Intl. Conf. on Robotics & Automation (ICRA)*, 2019, pp. 4790–4796.
- [7] J. Li and G. H. Lee, “Deepip2p: Image-to-point cloud registration via deep classification,” in *Proc. of the IEEE/CVF Conf. on Computer Vision and Pattern Recognition (CVPR)*, 2021, pp. 15 960–15 969.
- [8] S. Ren, Y. Zeng, J. Hou, and X. Chen, “Corri2p: Deep image-to-point cloud registration via dense correspondence,” *IEEE Trans. on Circuits and Systems for Video Technology (TCSVT)*, vol. 33, no. 3, pp. 1198–1208, 2022.
- [9] J. Sun, Z. Shen, Y. Wang, H. Bao, and X. Zhou, “Loftr: Detector-free local feature matching with transformers,” in *Proc. of the IEEE/CVF Conf. on Computer Vision and Pattern Recognition (CVPR)*, 2021, pp. 8922–8931.
- [10] W. Jiang, E. Trulls, J. Hosang, A. Tagliasacchi, and K. M. Yi, “Cotr: Correspondence transformer for matching across images,” in *Proc. of the IEEE/CVF Conf. on Computer Vision and Pattern Recognition (CVPR)*, 2021, pp. 6207–6217.
- [11] Z. Qin, H. Yu, C. Wang, Y. Guo, Y. Peng, and K. Xu, “Geometric transformer for fast and robust point cloud registration,” in *Proc. of the IEEE/CVF Conf. on Computer Vision and Pattern Recognition (CVPR)*, 2022, pp. 11 143–11 152.
- [12] V. Lepetit, F. Moreno-Noguer, and P. Fua, “Epnp: An accurate  $O(n)$  solution to the p n p problem,” *Intl. Journal of Computer Vision (IJCV)*, vol. 81, pp. 155–166, 2009.
- [13] M. A. Fischler and R. C. Bolles, “Random sample consensus: a paradigm for model fitting with applications to image analysis and automated cartography,” *Communications of the ACM*, vol. 24, no. 6, pp. 381–395, 1981.
- [14] D. G. Lowe, “Distinctive image features from scale-invariant keypoints,” *Intl. Journal of Computer Vision (IJCV)*, vol. 60, pp. 91–110, 2004.
- [15] E. Rublee, V. Rabaud, K. Konolige, and G. Bradski, “Orb: An efficient alternative to sift or surf,” in *Proc. of the IEEE/CVF Intl. Conf. on Computer Vision (ICCV)*, 2011, pp. 2564–2571.
- [16] DeTone, Daniel and Malisiewicz, Tomasz and Rabinovich, Andrew, “Superpoint: Self-supervised interest point detection and description,” in *Proc. of the IEEE/CVF Conf. on Computer Vision and Pattern Recognition Workshops (CVPRW)*, 2018, pp. 224–236.
- [17] P.-E. Sarlin, D. DeTone, T. Malisiewicz, and A. Rabinovich, “Superglue: Learning feature matching with graph neural networks,” in *Proc. of the IEEE/CVF Conf. on Computer Vision and Pattern Recognition (CVPR)*, 2020, pp. 4938–4947.
- [18] Q. Zhou, T. Sattler, and L. Leal-Taixe, “Patch2pix: Epipolar-guided pixel-level correspondences,” in *Proc. of the IEEE/CVF Conf. on Computer Vision and Pattern Recognition (CVPR)*, 2021, pp. 4669–4678.
- [19] H. Deng, T. Birdal, and S. Ilic, “Ppf-foldnet: Unsupervised learning of rotation invariant 3d local descriptors,” in *Proc. of the Europ. Conf. on Computer Vision (ECCV)*, 2018, pp. 602–618.
- [20] Z. Gojcic, C. Zhou, J. D. Wegner, and A. Wieser, “The perfect match: 3d point cloud matching with smoothed densities,” in *Proc. of the IEEE/CVF Conf. on Computer Vision and Pattern Recognition (CVPR)*, 2019, pp. 5545–5554.
- [21] H. Wang, Y. Liu, Q. Hu, B. Wang, J. Chen, Z. Dong, Y. Guo, W. Wang, and B. Yang, “Roreg: Pairwise point cloud registration with oriented descriptors and local rotations,” *IEEE Trans. on Pattern Analysis and Machine Intelligence (TPAMI)*, 2023.
- [22] H. Yu, F. Li, M. Saleh, B. Busam, and S. Ilic, “Cofinet: Reliable coarse-to-fine correspondences for robust pointcloud registration,” *Proc. of the Advances in Neural Information Processing Systems (NIPS)*, vol. 34, pp. 23 872–23 884, 2021.
- [23] J. Levinson and S. Thrun, “Automatic online calibration of cameras and lasers,” in *Proc. of Robotics: Science and Systems (RSS)*, vol. 2, no. 7, 2013.
- [24] Y. Liao, J. Li, S. Kang, Q. Li, G. Zhu, S. Yuan, Z. Dong, and B. Yang, “Se-calib: Semantic edges based lidar-camera boresight online calibration in urban scenes,” *IEEE Trans. on Geoscience and Remote Sensing (TGRS)*, 2023.
- [25] Q. Zhang and R. Pless, “Extrinsic calibration of a camera and laser range finder (improves camera calibration),” in *Proc. of the IEEE/RSJ Intl. Conf. on Intelligent Robots and Systems (IROS)*, vol. 3, 2004, pp. 2301–2306.
- [26] D. Scaramuzza, A. Harati, and R. Siegwart, “Extrinsic self calibration of a camera and a 3d laser range finder from natural scenes,” in *Proc. of the IEEE/RSJ Intl. Conf. on Intelligent Robots and Systems (IROS)*, 2007, pp. 4164–4169.
- [27] Y. Zhong, “Intrinsic shape signatures: A shape descriptor for 3d object recognition,” in *Proc. of the Int. Conf. on Computer Vision Workshops (ICCVW)*, 2009, pp. 689–696.
- [28] K. He, X. Zhang, S. Ren, and J. Sun, “Deep residual learning for image recognition,” in *Proc. of the IEEE/CVF Conf. on Computer Vision and Pattern Recognition (CVPR)*, 2016, pp. 770–778.
- [29] H. Thomas, C. R. Qi, J.-E. Deschaud, B. Marcotegui, F. Goulette, and L. J. Guibas, “Kpconv: Flexible and deformable convolution for point clouds,” in *Proc. of the IEEE/CVF Intl. Conf. on Computer Vision (ICCV)*, 2019, pp. 6411–6420.
- [30] W. Zhang, Z. Huang, G. Luo, T. Chen, X. Wang, W. Liu, G. Yu, and C. Shen, “Topformer: Token pyramid transformer for mobile semantic segmentation,” in *Proc. of the IEEE/CVF Conf. on Computer Vision and Pattern Recognition (CVPR)*, 2022, pp. 12 083–12 093.
- [31] Q. Wan, Z. Huang, J. Lu, G. Yu, and L. Zhang, “Seaformer: Squeeze-enhanced axial transformer for mobile semantic segmentation,” in *Proc. of the Int. Conf. on Learning Representations (ICLR)*, 2023.
- [32] H. Yu, Z. Qin, J. Hou, M. Saleh, D. Li, B. Busam, and S. Ilic, “Rotation-invariant transformer for point cloud matching,” in *Proc. of the IEEE/CVF Conf. on Computer Vision and Pattern Recognition (CVPR)*, 2023, pp. 5384–5393.
- [33] K. Wu, H. Peng, M. Chen, J. Fu, and H. Chao, “Rethinking and improving relative position encoding for vision transformer,” in *Proc. of the IEEE/CVF Intl. Conf. on Computer Vision (ICCV)*, 2021, pp. 10 033–10 041.
- [34] Y. Sun, C. Cheng, Y. Zhang, C. Zhang, L. Zheng, Z. Wang, and Y. Wei, “Circle loss: A unified perspective of pair similarity optimization,” in *Proc. of the IEEE/CVF Conf. on Computer Vision and Pattern Recognition (CVPR)*, 2020, pp. 6398–6407.
- [35] A. Geiger, P. Lenz, and R. Urtasun, “Are we ready for autonomous driving? the kitti vision benchmark suite,” in *Proc. of the IEEE/CVF Conf. on Computer Vision and Pattern Recognition (CVPR)*, 2012, pp. 3354–3361.
- [36] B. Wang, C. Chen, Z. Cui, J. Qin, C. X. Lu, Z. Yu, P. Zhao, Z. Dong, F. Zhu, N. Trigoni *et al.*, “P2-net: Joint description and detection of local features for pixel and point matching,” in *Proc. of the IEEE/CVF Intl. Conf. on Computer Vision (ICCV)*, 2021, pp. 16 004–16 013.
- [37] A. Dosovitskiy, L. Beyer, A. Kolesnikov, D. Weissenborn, X. Zhai, T. Unterthiner, M. Dehghani, M. Minderer, G. Heigold, S. Gelly *et al.*, “An image is worth 16x16 words: Transformers for image recognition at scale,” in *Proc. of the Int. Conf. on Learning Representations (ICLR)*, 2021.